

# An improved artificial neural network for a direct-power control based on instantaneous power-ripple minimization of the shunt active-power filter

Mohamed Haithem Lazreg<sup>1</sup>, Abderrahim Bentaallah<sup>2</sup>, Hamza Mesai-Ahmed<sup>2,3</sup>, Youcef Djeriri<sup>2</sup>

<sup>1</sup> Laboratoire d'Automatique de Tlemcen (LAT), Université de Tlemcen, Algérie.

<sup>2</sup> Laboratoire ICEPS, Université Djillali Liabès, Sidi Bel-Abbès, Algérie.

<sup>3</sup> CISE - Electromechatronic Systems Research Centre, University of Beira Interior, Covilhã, Portugal

E-mail: mohamedhaithem.lazreg@univ-tlemcen.dz

**Abstract.** The paper presents a method for a direct-power control (DPC) based on Artificial Neural Networks (ANN) applied to a shunt active-power filter (SAPF). The aim is to improve the performance of conventional controls. SAPF is one of the most advanced pollution control solutions. DPC is a high-performance control for PWM converters based on the instantaneous-power theory. However, the presented control has some drawbacks, such as the presence of ripples in the current. To improve the performance of the system to be controlled, artificial neural networks are applied to the conventional control. To achieve the objective, DPC-ANN is combined with conventional DPC using MATLAB/Simulink, Simulation results show a very satisfactory performance.

**Keywords:** Shunt Active-Power Filter (SAPF); Direct-Power Control (DPC); Artificial Neural Networks (ANN); Harmonics compensation; Nonlinear load.

## Uporaba umetnih nevronske mreže za krmiljenje z neposrednim nadzorom porabe moči

Članek predstavlja krmiljenje z neposrednim nadzorom porabe moči (DPC), ki temelji na umetnih nevronske mrežah (ANN). Cilj predlaganega krmiljenja je izboljšati učinkovitost v primerjavi z običajnimi krmilniki. Krmiljenje DPC predstavlja visokozmogljivo strategijo krmiljenja za pretvornike PWM, ki temelji na trenutni porabi moči. Za ta pristop je značilno nihanje električnega toka. Z namenom izboljšanja delovanja sistema smo uporabili umetne nevronske mreže. Pravilnost predlagane metode smo potrdili v postopku simulacije.

## 1 INTRODUCTION

After its production, electric energy has to be maintained and monitored to avoid disturbances during its transport. The origin of the most significant disturbances in the electric power networks is on the consumer side. They are caused by the proliferation of non-linear loads, such as static converters, computer equipments, air-conditioning units, and lighting devices. These devices absorb non-sinusoidal currents and thus introduce a harmonic pollution into the currents and voltages of electric distribution networks [1].

For these reasons, the focus of the current concerns is on filtering the current and voltage distortions for both suppliers and users of electric energy. The shunt active-power filters (SAPF) are currently the most suitable pollution control solution. Their response is

instantaneous and they automatically adapt to changes in the disturbances introduced by the electric network loads [2].

In the presence of a non-linear load, harmonics are superimposed on the source current creating a polluted current. The injection of compensation currents into the electric network by SAPF allows the initial form of the current to be restored.

The most commonly used control strategies are Voltage-Oriented Control (VOC) [3], and Virtual-Flux-Oriented Control (VFOC) [4]. They assure a high dynamic and static performance by using an internal current-control loop. They have become widely used and are being constantly improved.

Since the combination of a grid-active filter-pollutant load results in a non-linear system, it makes sense to use a direct-power control (DPC). It is based on an instantaneous control of the active and reactive power. In this control, the current control loops and the modulation block are eliminated, and the switch states of the converter selected from a switching table are based on instantaneous errors between the estimated active and reactive power and their reference values [5].

The major DPC drawback is the presence of ripples in the current waveform. To avoid them, modern artificial intelligence techniques are used, such as the fuzzy control [6], genetic algorithms [7], and neural networks.

The aim of our work is to simultaneously improve the SAPF performance in terms of residual distortion, allow it to compensate for the reactive power, enable it to selectively compensate for harmonics and to reduce the complexity of the computing architecture.

The paper is organized as follows. Section 2 presents the SAPF model. Section 3 describes the control method based on a conventional DPC modelling. Section 4 presents DPC based on Artificial Neural Networks (DPC-ANN). Section 5 discusses the simulation results made with Matlab/Simulink. Section 6 draws conclusions of our work.

## 2 SAPF MATHEMATICAL MODEL

Using a model of the active filter in a three-phase reference frame and applying the direct Concordia transform, the SAPF model in the stationary reference frame ( $\alpha\beta$ ) is given by:

$$\begin{bmatrix} P_f \\ Q_f \end{bmatrix} = \begin{bmatrix} v_{f\alpha} & v_{f\beta} \\ -v_{f\beta} & v_{f\alpha} \end{bmatrix} \begin{bmatrix} i_{f\alpha} \\ i_{f\beta} \end{bmatrix} \quad (\text{Eq 1})$$

The mathematical model of the shunt active power for power control is given by:

$$\frac{dP_f}{dt} = \frac{1}{L_f} (-R_f P_f + V_{f\alpha})$$

$$\frac{dQ_f}{dt} = \frac{1}{L_f} (-R_f Q_f + V_{f\beta}) \quad (\text{Eq 2})$$

$$\frac{dV_{dc}}{dt} = \frac{P_{dc}}{V_{dc} C_{dc}}$$

Where  $P_f$  and  $Q_f$  are the active and reactive filter power, respectively,  $R_f$  and  $L_f$  are the SAPF filter resistance and inductance, respectively.

Where:

$$V_{f\alpha} = v_{\alpha} v_{f\alpha} + v_{\beta} v_{f\beta} - (v_{\alpha}^2 + v_{\beta}^2) \quad (\text{Eq 3})$$

$$V_{f\beta} = -v_{\beta} v_{f\alpha} + v_{\alpha} v_{f\beta}$$

The energy storage on the DC side is often done by a capacitive storage system represented by capacitor  $C_{dc}$  which plays the role of DC voltage source  $V_{dc}$ . The choice of the storage system parameters ( $C_{dc}$  and  $V_{dc}$ ) effects the SAPF dynamics and compensation quality, respectively [8].

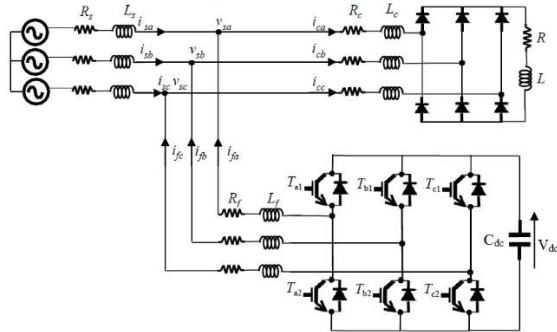


Figure 1. SAPF power circuit.

## 3 CONVENTIONAL DPC THEORY

The DPC main idea, which was first proposed by Ohnishi in 1991 [9] and later developed by Noguchi and Takahachi in 1998 [10], is similar to the direct torque control (DTC) of induction machines. Instead of the flux and torque, the instantaneous active and reactive power are chosen as the quantities to be controlled [11]. Figure 2 shows an overall DPC configuration applied to SAPF.

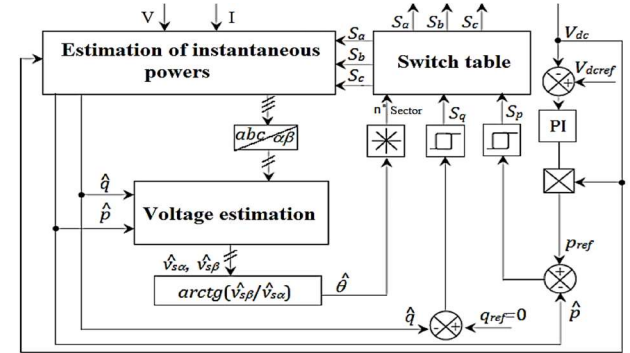


Figure 2. General configuration of the conventional DPC.

### 3.1 Estimation of the instantaneous power

The instantaneous active power is defined by the scalar product between the line currents and voltages. Where the reactive power is defined by the vector product between them. The complex apparent power can be expressed by the following expression [12]:

$$\bar{S} = p + jq \quad (\text{Eq 4})$$

$$\bar{S} = v_{sa} \cdot i_{sa} + v_{sb} \cdot i_{sb} + v_{sc} \cdot i_{sc} + \frac{1}{\sqrt{3}} [(v_{sb} - v_{sc}) \cdot i_{sa} + (v_{sc} - v_{sa}) \cdot i_{sb} + (v_{sa} - v_{sb}) \cdot i_{sc}] \quad (\text{Eq 5})$$

Where  $v_s$  is the instantaneous voltage of the network and  $i_s$  is the instantaneous line current.

However, Eq.4 requires the knowledge of the grid voltages. Therefore, it is necessary to express the powers by other expressions independent of the network voltages. Thus, the expressions that estimate the instantaneous active and reactive power without capturing the voltages are [13]:

$$\bar{p} = L \left( \frac{di_{sa}}{dt} + \frac{di_{sb}}{dt} + \frac{di_{sc}}{dt} \right) + V_{dc} (S_a i_{sa} + S_b i_{sb} + S_c i_{sc}) \quad (\text{Eq 6})$$

$$\bar{q} = \frac{1}{\sqrt{3}} \left[ L \left( \frac{di_{a}}{dt} i_{sc} + \frac{di_{c}}{dt} i_{sa} \right) - V_{dc} (S_a (i_{sb} - i_{sc}) + S_b (i_{sc} - i_{sa}) + S_c (i_{sa} - i_{sb})) \right] \quad (\text{Eq 7})$$

The first part of both expressions represents the power of the line inductors. Their internal resistance is negligible because the active power dissipated in these resistors is actually much lower than the power [14]. The second part represents the SAPF output power. Eqs 6 and 7 are functions of the states of switches  $S_a$ ,  $S_b$ ,  $S_c$ . The knowledge of line inductance  $L$  is also necessary to estimate the powers.

### 3.2 Voltage calculation

As the sector number calculation is based on the position of the voltage vector, the line voltage is calculated [15]. The following expression gives line currents  $i_{sa}$ ,  $i_{sb}$ ,  $i_{sc}$  in stationary coordinates  $\alpha$ ,  $\beta$ :

$$\begin{bmatrix} i_{s\alpha} \\ i_{s\beta} \end{bmatrix} = \sqrt{\frac{2}{3}} \begin{bmatrix} 1 & -\frac{1}{2} & -\frac{1}{2} \\ 0 & \frac{\sqrt{3}}{2} & -\frac{\sqrt{3}}{2} \end{bmatrix} \begin{bmatrix} i_{sa} \\ i_{sb} \\ i_{sc} \end{bmatrix} \quad (\text{Eq 8})$$

Both the active and reactive-power equations can be written in a matrix form as follows:

$$\begin{bmatrix} \hat{p} \\ \hat{q} \end{bmatrix} = \begin{bmatrix} v_{s\alpha} & v_{s\beta} \\ v_{s\beta} & -v_{s\alpha} \end{bmatrix} \begin{bmatrix} i_{s\alpha} \\ i_{s\beta} \end{bmatrix} \quad (\text{Eq 9})$$

The voltage can be estimated by the following equation:

$$\begin{bmatrix} \hat{v}_{s\alpha} \\ \hat{v}_{s\beta} \end{bmatrix} = \frac{1}{i_{s\alpha}^2 + i_{s\beta}^2} \begin{bmatrix} i_{s\alpha} & -i_{s\beta} \\ i_{s\beta} & i_{s\alpha} \end{bmatrix} \begin{bmatrix} \hat{p} \\ \hat{q} \end{bmatrix} \quad (10)$$

Components  $\hat{v}_{s\alpha}$  and  $\hat{v}_{s\beta}$  being projections of voltage vector  $v_s$  onto the  $\alpha$  and  $\beta$  axis, respectively, the three voltage vectors in a three-phase plant can be represented by single voltage vector  $\hat{v}_s$  in a two-phase plane  $\alpha$ - $\beta$  which rotates with the pulsation of  $\omega=2\pi f$  in a circle of radius of  $\sqrt{3/2} \cdot V_m$  [16].

$f$  is the frequency of the network.

$V_m$  is the amplitude of three-phase voltages.

### 3.3 Switching table

Digital error signals  $S_p$  and  $S_q$  and the sector number are the inputs to the switching table where switching states  $S_a$ ,  $S_b$  and  $S_c$  are stored [17].

The optimal switching state can be chosen in each switching state according to a combination of digital signals  $S_p$  and  $S_q$  and the sector number. That is, the optimal switching state is chosen so that the active-power error can be restricted to a hysteresis band of width of  $2h_p$ , and similarly for the reactive-power error to a band of the width of  $2h_q$ .

Switching-table synthesis is based on the signs of the active and reactive-power derivatives in each sector [18]. For each sector, the change in the reactive power is positive for three vectors, negative for three vectors, and zero for  $V_0$ ,  $V_7$ . The sign of the active power change is positive for four vectors and negative for two or three vectors. For all sectors, the switching table is shown in Table 1.

Table 1. DPC switching table

$S_p$	$S_q$	$\gamma_1$	$\gamma_2$	$\gamma_3$	$\gamma_4$	$\gamma_5$	$\gamma_6$	$\gamma_7$	$\gamma_8$	$\gamma_9$	$\gamma_{10}$	$\gamma_{11}$	$\gamma_{12}$
1	0	$V_5$	$V_5$	$V_6$	$V_6$	$V_1$	$V_1$	$V_2$	$V_2$	$V_3$	$V_3$	$V_4$	$V_4$
1	1	$V_3$	$V_3$	$V_4$	$V_4$	$V_5$	$V_5$	$V_6$	$V_6$	$V_1$	$V_1$	$V_2$	$V_2$
0	0	$V_6$	$V_1$	$V_1$	$V_2$	$V_2$	$V_3$	$V_3$	$V_4$	$V_4$	$V_5$	$V_5$	$V_6$
0	1	$V_1$	$V_2$	$V_2$	$V_3$	$V_3$	$V_4$	$V_4$	$V_5$	$V_5$	$V_6$	$V_6$	$V_1$

### 3.4 DC-link voltage control with the conventional method

The DC voltage is controlled by a PI-type controller which corrects the error between the measured DC voltage and its reference. The product of the reference DC current and DC voltage gives the reference active power.

The corresponding transfer function is given by:

$$F(s) = k_p + \frac{k_i}{s} \quad (\text{Eq 11})$$

where  $s$  is the Laplace operator.

Figure 3 shows the DC voltage control using a PI corrector.

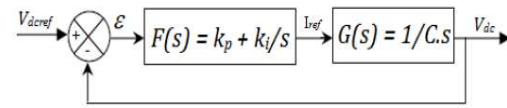


Figure 3. PI controller to control the DC-link voltage.

## 4 DPC ARTIFICIAL NEURAL NETWORKS

One of the challenges for humans today is to copy nature and reproduce its own patterns of reasoning and behaviour. The neural network architecture is the way in which neurons are interconnected to form a network. When the structure of a neural network is fixed, a learning process must be chosen, by which the weights will be adjusted in order to satisfy an optimisation criterion [19]. A satisfactory solution can only be obtained if the complexity of the neural network is adapted to the problem to be solved [20].

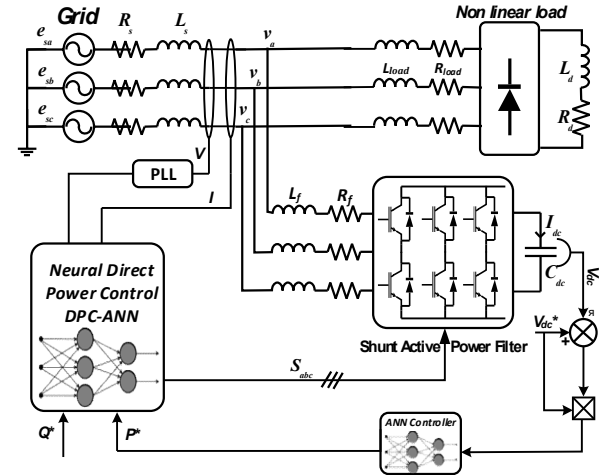


Figure 4. Block diagram of the proposed DPC-ANN for SAPF.

In our study, we use the perceptron neural networks. They are well suited to our application because of their simplicity of implementation and parallel computation, which makes online learning more efficient [21].

The neural network structure which replaces the switching table in conventional DPC of SAPF and the voltage controller ( $V_{dc}$ ) by another ANN are shown in Figure 4.

#### 4.1 DC-link voltage control based on ANN

In our study, the Adaline neural networks are used. They are a special type of the multilayer network which has a very simple architecture (one input layer and one output layer). They are very efficient in signal estimation tasks and in their implementation. Moreover, their operation allows a better exploitation of their characteristics [22]. The Adaline (ADAPtive LINear Element/ADAPtive LInear NEuron) neural network belongs to the Perceptron family.

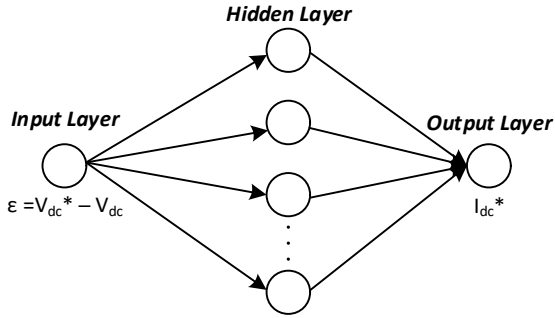


Figure 5. Neural network structure of the DC voltage controller.

A schematic diagram of an Adaline network is given in Figure 5. Estimated output  $y(t)_{est}$  of reference signal  $y^*(t)$  is set up by the following linear relation:

$$y(t)_{est} = W^T(t) \cdot X(t) \quad (\text{Eq 12})$$

where  $W^T(t)$  is a vector of the weights estimated by Adaline and  $X(t)$  is the vector of inputs consisting of the known components of reference signal  $y(t)$ .

Thus:

$$W^T = [W_0(t) \ W_1(t) \ W_2(t) \ \dots \ W_{n-1}(t) \ W_n(t)] \quad (\text{Eq 13})$$

$$X(t) = [1 \ x_1(t) \ x_2(t) \ \dots \ x_{n-1}(t) \ x_n(t)] \quad (\text{Eq 14})$$

#### 4.2 SWITCHING TABLE based on ANN

The structure of the SAPF direct neural power control (DPC-ANN) is shown in Figure 6. The switching table is replaced by a neural controller. The inputs are active power error  $S_p$ , reactive power  $S_q$ , and sector number  $N$ . The outputs are pulses  $S_a$ ,  $S_b$ ,  $S_c$  which control the inverter switches.

In order to generate an ANN controller by Matlab/Simulink, 30 hidden layers and three output layers with activation functions of the type "tansig" and "purelin" are used (Table 2).

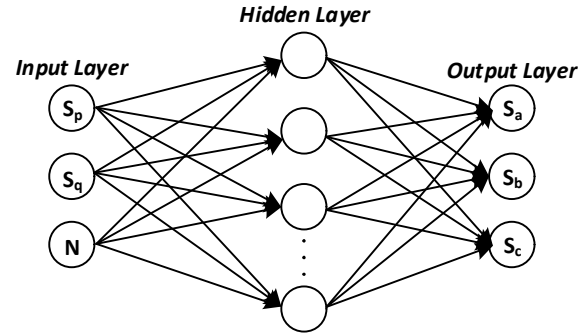


Figure 6. Replacement of the switching table by a neural network structure.

Updating the network weights and biases is performed by a backpropagation algorithm termed the Levenberg-Marquardt (LM) algorithm.

Table 2. Properties of the LM algorithm.

LM parameters	Values
Number of the hidden layers	30
Learning step	0.005
Display step (displaying the error in pieces)	50
Number of iterations (epochs)	2000
Convergence acceleration coefficient (mc)	0.9
Error (goal)	0
Activation functions	Tansig, Purelin

## 5 SIMULATION RESULTS

To validate the effectiveness of the presented control strategy, a system simulation controlled by conventional DPC and DPC-ANN is performed under the MATLAB\SIMULINK environment. The parameters of the simulated system are given in Table 3.

Table 3. The parameters of the simulated system

<b>Power grid</b>	$V_s = 400V, R_s = 0\Omega, L_s = 400\mu H$
<b>Pollutant load (Graëtz bridge with thyristors)</b>	$R_{ch} = 0\Omega, L_{ch} = 566\mu H$ $R_d = 7\Omega, L_d = 1mH$
<b>Shunt Active-Power Filter</b>	$R_f = 32m\Omega, L_f = 500\mu H, V_{dc} = 700V$

The simulation is carried out in two scenarios:

#### 5.1 First scenario:

The simulation is performed in three steps:

- $t \in [0; 0.06]$  the electric network supplies a linear inductive load,
- $t \in [0.06; 0.12]$  elimination of the load,
- $t \in [0.12; 0.2]$  the voltage source feeds a non-linear load.

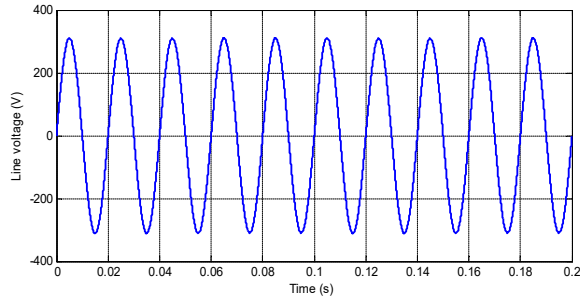


Figure 7. Source voltage  $V_{sa}$  [V].

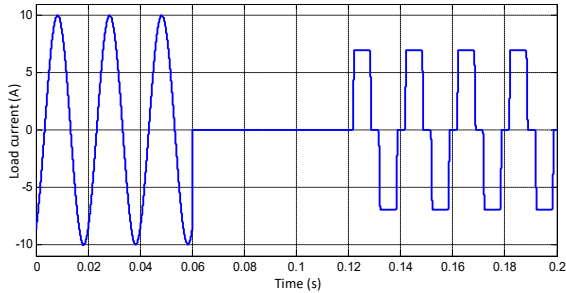


Figure 8. Current absorbed by a non-linear load [A].

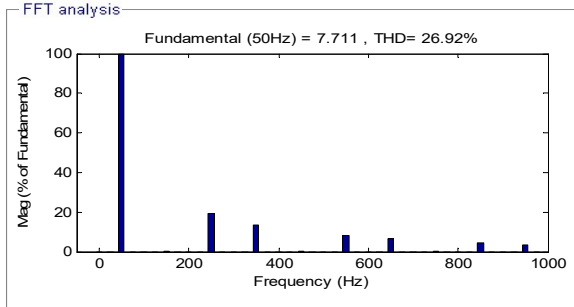


Figure 9. Current harmonic spectrum.

These three steps can be clearly seen by observing the waveform of the current absorbed by the load (Figure 8).  
 - For a linear inductive load it is well seen that the current lags behind the phase with respect to the voltage (Figure 7).

- A zero current corresponds to a charge removal between 0.06s and 0.12s.

- The distorted form of the current that appears between 0.12s and 0.2s corresponds to a non-linear load represented by a three-phase bridge rectifier with six diodes. Its harmonic spectrum of the value of THD= 26.92% is shown in Figure 9.

The figures below show the waveforms of the different quantities to be analysed in a simulation for conventional DPC and DPC-ANN.

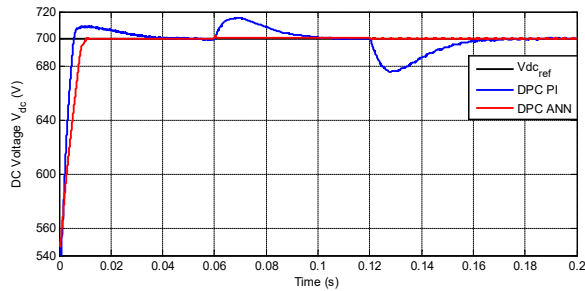


Figure 10. DC voltage  $V_{dc}$  [V].

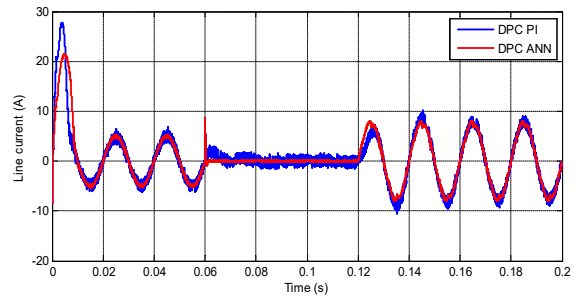


Figure 11. Source current  $i_{sa}$  [A].

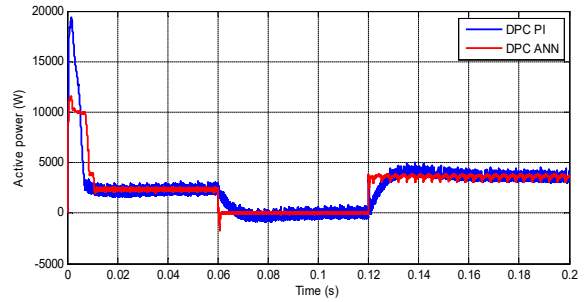


Figure 12. Instantaneous active power [W].

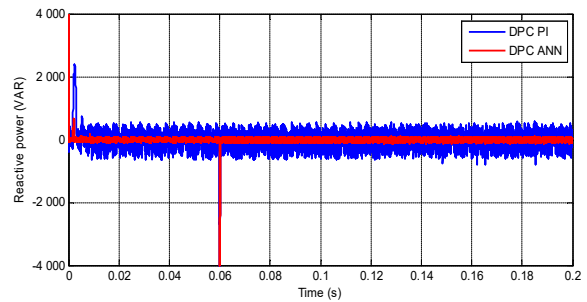


Figure 13. Instantaneous reactive power [VAR].

As seen from the above figures, it is noted that DPC-ANN improves the grid current harmonic content (Figure 11). In the used control technique, the active filter has a double role: compensation of the reactive power (Figure 13) in the steady-state (at  $f=50\text{Hz}$ ) and attenuation of the dominant harmonics by pushing them toward higher frequencies.

Figure 10 shows that the DPC technique offers some extra speed and robustness to the system response compared to the conventional DPC technique. The figures clearly illustrate that the main advantage of using the neural network in the development of the switching table and DC voltage control, i.e., are significantly minimised ripples.

### 5.2 Second scenario

The DC voltage control system as well as the neural network-enhanced DPC strategy are tested following a step change in the DC voltage at  $t=0.1\text{s}$  from 700V to 750V by using an inductive load (Figures 14 - 17).

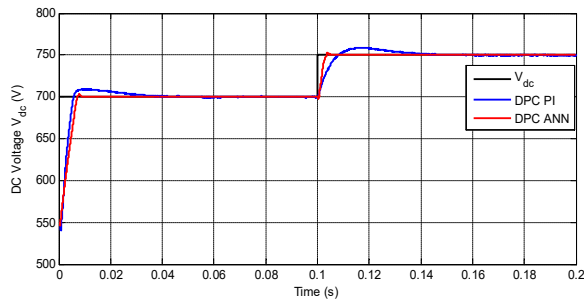
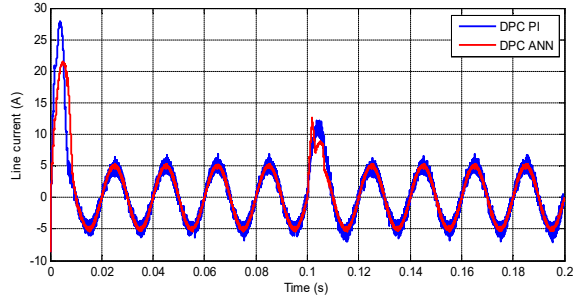
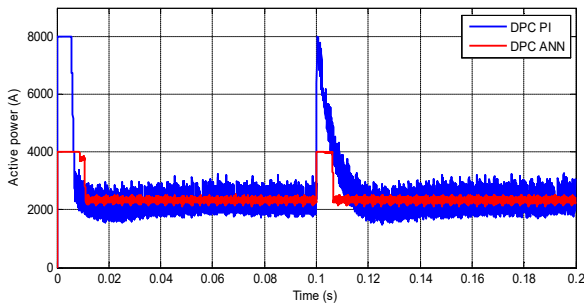
Figure 14. DC voltage  $V_{dc}$  [V].Figure 15. Source current  $i_{sa}$  [A].

Figure 16. Instantaneous active power [W].

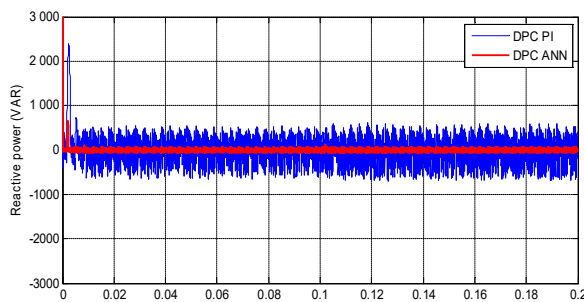


Figure 17. Instantaneous reactive power [VAR].

Figure 14 shows that the DC voltage tracks to the set point well and that when using an artificial neural network, the system becomes more stable compared to the system with a conventional control. The overshoot and response time are reduced. Figures 16 and 17 show the line active-and reactive-power waveforms. Figure 16 shows that when the DC voltage reaches its new reference value, the active power increases and so does also the line current (Figure 15). In the case of DPC-ANN, the power increase is limited to prevent the system from being subjected to a dangerous overcurrent. In Figure 17, the reactive power is significantly lower in DPC-ANN than in conventional DPC.

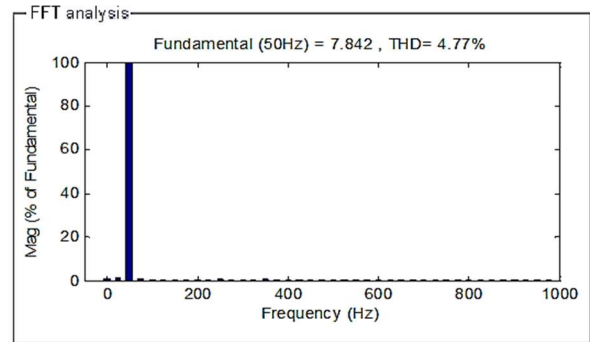


Figure 18. Current harmonic spectrum (conventional DPC).

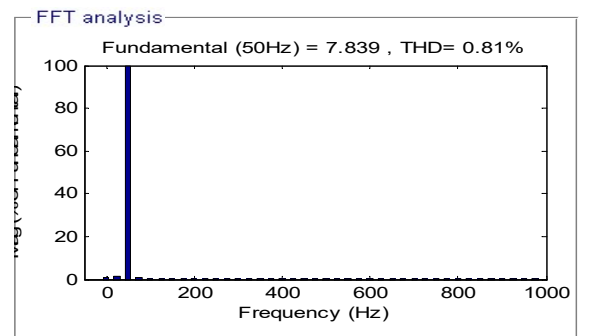


Figure 19. Current harmonic spectrum (DPC-ANN).

The harmonic spectrum of the source current after compensation is for the two techniques shown in Figures 18 and 19. The Total Harmonic Distortion (THD) before compensation is 26.92% and after its it is reduced to 0.81% for DPC-ANN compared to 4.77% for conventional DPC.

## 6 CONCLUSION

The paper presents a new technique to control the direct power. It used an artificial neural network instead of a conventional switching table and controls the DC voltage by a neural network controller.

The presented DPC based on an artificial neural network provides a good response, reduces the instantaneous power ripples, enables an excellent DC voltage control and a good performance and minimises harmonic disturbances. The simulation results show that DPC-ANN out performs the conventional control. THD is reduced from 26.92% to 0.81%, these ensuring a very good power quality compliably with the specifications of the IEEE 519-1992 and IEC 61000.3-2 standard.

## REFERENCES

- [1] M. Rasoul, F. Alan, L. Yunwei, "Adaptive control of an active power filter for harmonic suppression and power factor correction", *International Journal of Dynamics and Control*, 10(4), pp. 473–482, 2022.
- [2] R. Kumar, H.O. Bansal, "Real-time implementation of adaptive PV-integrated SAPF to enhance power quality", *International Transactions on Electrical Energy Systems*, 29(1), pp. 1-22, 2019.
- [3] F. Alireza, M. S. Masoum, "Adaptive Space-Vector Hysteresis-Based Control with Constant Switching-Frequency for Three-Level Shunt Active Power Filters", *Intelligent Industrial Systems*, 2(4), pp. 319–334, 2016.

- [4] S. S. Lee, Y. E. Heng, "Optimal VF-PDPC of grid connected inverter under unbalanced and distorted grid voltages", *Electric Power Systems Research*, 140, pp. 1–8, 2016.
- [5] K. B. Prasanta, S. Gauri, K. S. Pradeepta, "Investigations on Split-Source Inverter Based Shunt Active Power Filter Integrated Microgrid System for Improvement of Power Quality Issues", *Journal of Electrical Engineering & Technology*, 17(1), pp. 2025–2047, 2022.
- [6] V. Narasimhulu, D. V. Ashok Kumar, Ch. Sai Babu, "Fuzzy Logic Control of SLMC-Based SAPF Under Nonlinear Loads", *International Journal of Fuzzy Systems*, 22(2), pp. 428–437, 2020.
- [7] T. Kaya, H. Guler, "A hybrid genetic algorithm for analog active filter component selection", *AEU - International Journal of Electronics and Communications*, 86, pp. 1–7, 2018.
- [8] R. Kumar, H.O. Bansal, "Shunt active power filter: Current status of control techniques and its integration to renewable energy sources", *Sustainable Cities and Society*, 42, pp. 574–592, 2018.
- [9] T. Ohnishi, "Three phase PWM converter/inverter by means of instantaneous active and reactive power control", *International Conference on Industrial Electronics, Control and Instrumentation*, Kobe, Japan, 28 October 1991.
- [10] T. Noguchi, H. Tomiki, S. Kondo, I. Takahashi, "Direct power control of PWM converter without power source voltage sensors", *IEEE Transactions on Industry Applications*, 34(3), pp. 473–479, 1998.
- [11] M. H. Lazreg, A. Bentaallah, "Sensorless Speed Control of Double Star Induction Machine with Five Level DTC Exploiting Neural Network and Extended Kalman Filter", *Iranian Journal of Electrical and Electronic Engineering*, 15(1), pp. 142–150, 2019.
- [12] H. Medouche, H. Benalla, "Predictive model approach based direct power control for power quality conditioning", *International Journal of System Assurance Engineering and Management*, 8(1), pp. 1832–1848, 2017.
- [13] M. AlShabi, A. Elnady, "Recursive Smooth Variable Structure Filter for Estimation Processes in Direct Power Control Scheme Under Balanced and Unbalanced Power Grid", *IEEE Systems Journal*, 14(1), pp. 971–982, 2020.
- [14] L. Yushan, G. Baoming, A. Haitham, S. Hexu, "Model Predictive Direct Power Control for Active Power Decoupled Single-Phase Quasi-Z -Source Inverter", *IEEE Transactions on Industrial Informatics*, 12(4), pp. 1550–1559, 2016.
- [15] M. Pichan; M. Seyyedhosseini; H. Hafezi, "A New DeadBeat-Based Direct Power Control of Shunt Active Power Filter with Digital Implementation Delay Compensation", *IEEE Access*, 10(1), pp. 72866 - 72878, 2022.
- [16] Y. Gui, Q. Xu, F. Blaabjerg, H.Gong, "Sliding Mode Control With Grid Voltage Modulated DPC for Voltage Source Inverters Under Distorted Grid Voltage", *CPSS Transactions on Power Electronics and Applications*, 4(3), pp. 244–254, 2019.
- [17] K. Kulikowski, A. Sikorski, "New DPC Look-Up Table Methods for Three-Level AC/DC Converter", *IEEE Transactions on Industrial Electronics*, 63(12), pp. 7930–7938, 2016.
- [18] S. Gao, H. Zhao, Y. Gui, J. Luo, F. Blaabjerg, "Impedance Analysis of Voltage Source Converter Using Direct Power Control", *IEEE Transactions on Energy Conversion*, 36(2), pp. 831–840, 2021.
- [19] T. Hubana, M. Šarić, S. Avdaković, "High-impedance fault identification and classification using a discrete wavelet transform and artificial neural networks", *Elektrotehniški vestnik*, 85(3), pp.109–114, 2018.
- [20] R. A. De Marchi, P. S. Dainez, F. J. Von Zuben, E. Bim, "A Multilayer Perceptron Controller Applied to the Direct Power Control of a Doubly Fed Induction Generator", *IEEE Transactions on Sustainable Energy*, 5(2), pp. 498–506, 2014.
- [21] M. Iqbal, M. Jawad, M. H. Jaffery, S. Akhtar, M. N. Rafiq, "Neural Networks Based Shunt Hybrid Active Power Filter for Harmonic Elimination", *IEEE Access*, 9, pp. 69913–69925, 2021.
- [22] J. Fei, H. Wang, Y. Fang, "Novel Neural Network Fractional-Order Sliding-Mode Control with Application to Active Power Filter", *IEEE Transactions on Systems*, 52(6), pp. 3508–3518, 2021.

**Mohamed Haithem Lazreg** received his Master and Ph.D. degrees in Electrical Engineering in 2015 and 2019, respectively, from Djillali Liabes University, Sidi Bel Abbes, Algeria. Currently he is a senior lecturer at the Electrical Engineering Department, Faculty of Technology at University of Tlemcen, Algeria, and a member of the LAT Laboratory. His research activities include control of ac drives and sensorless, intelligent artificial control, wind and hybrid power systems.

**Abderrahim Bentaallah** received his BS, MSc. and Ph.D. degrees in Electrical Engineering from the Djillali Liabes University, Sidi Bel-Abbes, Algeria, in 1991, 2005 and 2009, respectively. He is currently a Professor of Electrical Engineering at the same university. He is a member of ICEPS. His research interest is in robust control of electric machines.

**Hamza Mesai-Ahmed** received his Ph.D. degree in Electrical Engineering in 2022 from Djillali Liabes University, Sidi Bel Abbes, Algeria. He is a Researcher member in the ICEPS Intelligent Control Electric Power System Laboratory, Sidi Bel Abbes, Algeria and also in CISE Electromechatronic Systems Research Centre, Covilhã, Portugal (<http://cise.ubi.pt>). From 2018 to 2019, he was an Invited Professor with the Department of Electrical Engineering, University of Eloued, Algeria. His main research interests in renewable energies, multiphase machine, fault diagnosis, model predictive and artificial intelligence control of power electronics.

**Youcef Djeriri**, received his Ph.D. degree in Electrical Engineering in 2015 from the Electrical Engineering Faculty of Djillali Liabes University at Sidi Bel-Abbes, Algeria. He is a member of the Intelligent Control & Electrical Power Systems (ICEPS) Research Laboratory. His research interests are in robust, advanced and intelligent control methods of AC drives associated with power electronic converters for renewable energy applications.